ELSEVIER

Effect of Inlet Geometry and Heating on the Fully Developed Friction Factor in the Transition Region of a Horizontal Tube

Lap-Mou Tam*
Afshin J. Ghajar
School of Mechanical and Aerospace Engineering,
Oklahoma State University,
Stillwater, Oklahoma 74078

■Pressure drop measurements were made with a differential pressure transducer in the fully developed region of a horizontal circular straight tube with reentrant, square-edged, and bell-mouth inlets under isothermal and nonisothermal (uniform wall heat flux) flow conditions. The inlet Reynolds number for the ethylene glycol–water mixtures throughout the experiments ranged from about 1000 to 17,000 to cover laminar, transition, and turbulent regimes. The isothermal fully developed friction factors showed that the range of Reynolds number values for which transition flow exists is about 2900–3500 for the reentrant inlet, 3100–3700 for the square-edged inlet, and 5100–6100 for the bell-mouth inlet. Different heat fluxes (3, 8, and 16 kW/m^2) were applied to the test section to investigate the effect of heating on the friction factor. The results indicated that the value of the fully developed friction factor increased with an increase in the heating rate for a fixed Reynolds number. Owing to the presence of secondary flow, the effect of heating on the friction factor was significant in the laminar and transition regions. This increase in friction factor caused an increase in the lower and upper limits of the isothermal transition boundaries. For example, for the 16 kW/m^2 heat flux, the transition boundaries increased to about 4100–5900 for the reentrant inlet, 4500–6400 for the square-edged inlet, and 7300–9600 for the bell-mouth inlet. Available correlations for the prediction of nonisothermal fully developed friction factors are compared with our experimental data. Correlations for the prediction of the nonisothermal fully developed friction factors in the laminar and transition regions for the three inlets are recommended. The effect of heating in these correlations was accounted for in terms of a bulk-to-wall-viscosity ratio expressed as a function of Prandtl and Grashof numbers. © Elsevier Science Inc., 1997

Keywords: *friction factor, isothermal, nonisothermal, transition region, circular tube, uniform wall heat flux*

INTRODUCTION

Most pipe flow friction analyses are performed subject to the assumption that the fluid properties do not vary with temperature throughout the flow field. In practical situations, this assumption is obviously an idealization, because the transport properties of most fluids vary with temperature and thus vary over the flow cross section of a tube. The general effect of the variation of the transport properties with temperature is to change the velocity profile, yielding a different friction factor from that which would be obtained if properties were constant.

The analytical investigation of the effect of property variations is a highly complicated task for various reasons. The variations of properties with temperature differ from one fluid to another, and sometimes it is impossible to express these variations in analytical form. For practical applications, a reliable and appropriate correlation based on the constant-property assumption can be modified or corrected or both so that it can be used when the variable-property effect becomes important.

In the literature, two methods of correcting constant-property correlations for the variable-property effect have

Address correspondence to Professor A. J. Ghajar, School of Mechanical and Aerospace Engineering, Oklahoma State University, Stillwater,OK 74078.

* Present address: Faculty of Science and Technology, University of Macau, P.O. Box 30001, Macau.

Experimental Thermal and Fluid Science 1997; 15:52–64

655 Avenue of the Americas, New York, NY 10010

0894-1777/97/$17.00
PII S0894-1777(97)00035-6

been employed: namely, the reference-temperature method and the property-ratio method. In the reference-temperature method, a characteristic temperature is chosen at which the properties appearing in nondimensional groups (C_f, Re, Pr, etc.) are evaluated so that the constant-property results at that temperature may be used to evaluate (predict) the variable-property behavior. In the property-ratio method, all properties are evaluated at the bulk temperature, and then all variable-property effects are lumped into a function of the ratio of one property evaluated at the bulk temperature to that property evaluated at the wall temperature. The property-ratio method is used most often in the literature.

For liquids, the variation of viscosity is responsible for most of the property effects. Therefore, the variable property friction factor in the property-ratio method for liquids is correlated by

$$C_f = C_{vp} = C_{cp}\left(\frac{\mu_b}{\mu_w}\right)^m, \qquad (1)$$

where μ_b is the viscosity evaluated at the bulk temperature, μ_w is the viscosity evaluated at the wall temperature, "cp" refers to the constant-property (isothermal) solution, "vp" refers to the variable-property (nonisothermal) solution, and the exponent m is a flow parameter.

Extensive theoretical and experimental investigations with variable properties have been reported in the literature for laminar and turbulent regions to obtain the value of the exponent m. These works and the available correlations have been reviewed in detail by Kakac [1]. Table 1 summarizes some of the typical isothermal and nonisothermal friction factor correlations. However, there is no information in the literature on the effect of heating on the fully developed friction factor in the transition region. The addition of heat influences the beginning and end of the transition region. Moreover, the type of inlet configuration also influences the transition range [2]. Therefore, the application of these correlations to tubes with a wide range of entrance disturbances subjected to different heat fluxes as opposed to wall temperatures should be investigated.

The purpose of this study was to create an accurate and broad pressure drop (friction factor) database across all flow regimes in the fully developed region of a horizontal circular tube fitted with three different inlet configurations (reentrant, square-edged, and bell-mouth). Experiments were conducted in all three flow regimes (laminar, transition, and turbulent) under isothermal and nonisothermal (three different uniform heat fluxes) flow conditions. The experimental data were used to investigate the effect of heat flux and inlet configuration on the fully developed friction factor in the transition region. In addition, the database was used to establish the validity of the nonisothermal correlations presented in Table 1 and the development of appropriate friction factor correlations.

EXPERIMENTS

A schematic diagram of the overall experimental apparatus and the pressure drop test section used for pressure drop experiments is shown in Fig. 1. The overall experimental setup shown was also used for heat transfer [7, 8] and intermittency factor [9] measurements. The pressure drop test section was a horizontal seamless 316 stainless steel circular tube with an inside diameter of 1.58 cm and an outside diameter of 1.91 cm. The total length of the test section was 6.10 m, providing a maximum length-to-diameter ratio (L/D) of 386. For investigating the effect of heating on the pressure drop measurements, the end connections of the pressure drop test section consisted of copper plates that were arc soldered with silver to the ends of the test section to secure a well-defined electric circuit through the end plates. Welding cables from a Lincoln DC-600 welder were attached to the copper plates to provide a uniform wall heat flux boundary condition to the pressure drop test section. The test section was insulated from the environment by using fiberglass pipe insulation and vapor-proof pipe tape. The total thickness of the insulation materials was about 3.18 cm. To ensure a uniform fluid bulk temperature at the exit of the test section, a mixing well that consisted of several baffles was used. A one-shell and two-tube pass heat exchanger was used to cool the fluid from the test section to a desirable inlet bulk temperature.

For pressure drop measurements, pressure taps were placed at the top on the outer surface of the wall at close intervals near the entrance and at greater intervals further downstream (see Fig. 2 for details). Twenty-one pressure tap stations were designated with one 0.198-cm-diameter hole drilled at each station. Each of the pressure tap holes

Table 1. Isothermal and Nonisothermal Fully Developed Friction Factor Correlations Used in This Study

Investigator	*Correlation*	*Flow Regime*
Isothermal:		
Classic Relation	$C_f = 16/\mathrm{Re}$	Laminar
Blasius [3]	$C_f = 0.0791\mathrm{Re}^{-0.25}$	Turbulent
Nonisothermal:		
Deissler [4]	$C_f = \frac{16}{\mathrm{Re}}\left(\frac{\mu_b}{\mu_w}\right)^m$ where $m = -0.58$	Laminar
Test [5]	$C_f = \frac{16}{\mathrm{Re}}\frac{1}{0.89}\left(\frac{\mu_b}{\mu_w}\right)^m$ where $m = 0.2$	Laminar
Allen and Eckert [6]	$C_f = 0.0791\mathrm{Re}^{-0.25}\left(\frac{\mu_b}{\mu_w}\right)^m$ where $m = -0.25$	Turbulent

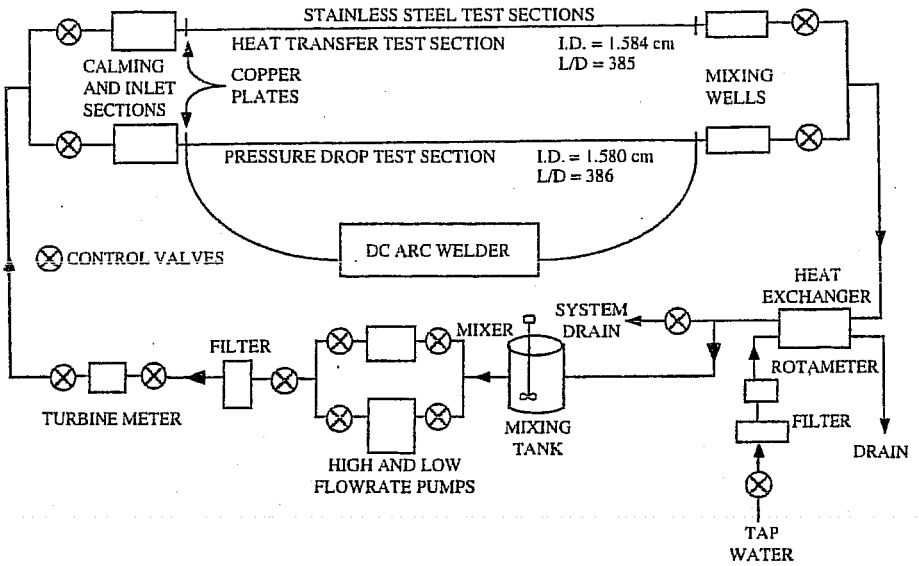

Figure 1. Diagram of the experimental setup.

was deburred with a special tool to ensure the characteristics of a smooth tube. For this study, pressure measurements were made with two Validyne model P305D and DP15 wet-wet differential pressure transducers. The pressure range of the model P305D pressure transducer is ± 22.2 in. of water. When the pressure was greater than ± 22.2 in. of water, the model DP15 pressure transducer was used because it is capable of handling pressures up to ± 55 in. of water. Both pressure transducers are accurate to $\pm 0.25\%$ of full scale, including linearity, hysteresis, and repeatability. The output of the transducers is bidirectional ± 5 V at 0.5 mA. The pressure transducers were connected to a personal computer through an A/D board. The calibration of the pressure transducers was checked regularly during the experiments. For sequential pressure drop measurements along the test section, a pressure tap manifold was used. This manifold made it possible to measure pressure drop from the reference pressure tap to any of the other 20 pressure taps. However, in this study, for pressure drop measurements in the fully developed region, only pressure taps at stations 16, 17, and 18 were used (see Fig. 2). Each pressure tap location was sampled at a user-defined number of samples, and the samples were taken by the computer, averaged, and recorded as the pressure reading for that location. The average of the pressure readings for the three pressure tap locations was used for the friction factor calculations. The variation between the pressure readings at each location was less than 1%. It is important to point out that the delay and number of samples used are very critical in the transition region. In the laminar and turbulent regions, the pressure reading is stable—hence, the delay and number of samples used are not critical. In these regions, the number of samples and delay used in this study were 1500 and 200 ms, resulting in a sampling rate of five samples per second. In the transition region, the pressure reading fluctuates, and a small delay and a large number of samples should be used to capture the characteristics of the transition region. In this region, the number of samples and delay used in this study were 12,000 and 100 ms, respectively. By delaying 100 ms between each sampling, a sampling rate of 10 samples per second was obtained.

To ensure a uniform velocity distribution at the entrance of the test section, the flow passed through a calming section and an inlet section (see Fig. 3). The calming section consisted of a 17.8-cm-outer-diameter acrylic plastic cylinder with three perforated circular acrylic plastic plates with an open area ratio of 0.312 (73 holes per plate, hole diameter 1.1 cm) followed by tightly packed soda straws (inside diameter 0.57 cm, length 10.2 cm, open area ratio 0.915) sandwiched between fine plastic mesh screens (strand diameter 0.03 cm, mesh width 0.14 cm, open area ratio 0.65). Two more fine plastic mesh

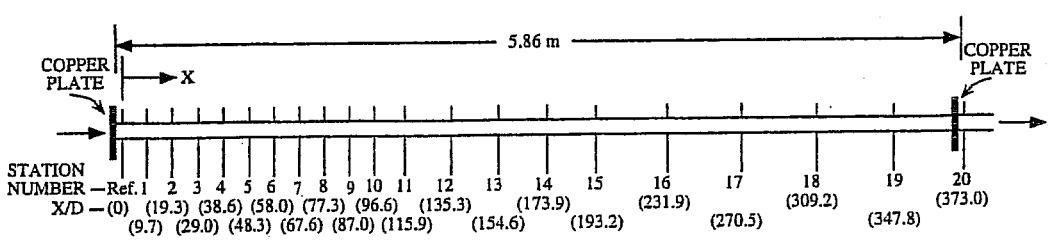

Figure 2. Pressure drop test section pressure tap distribution.

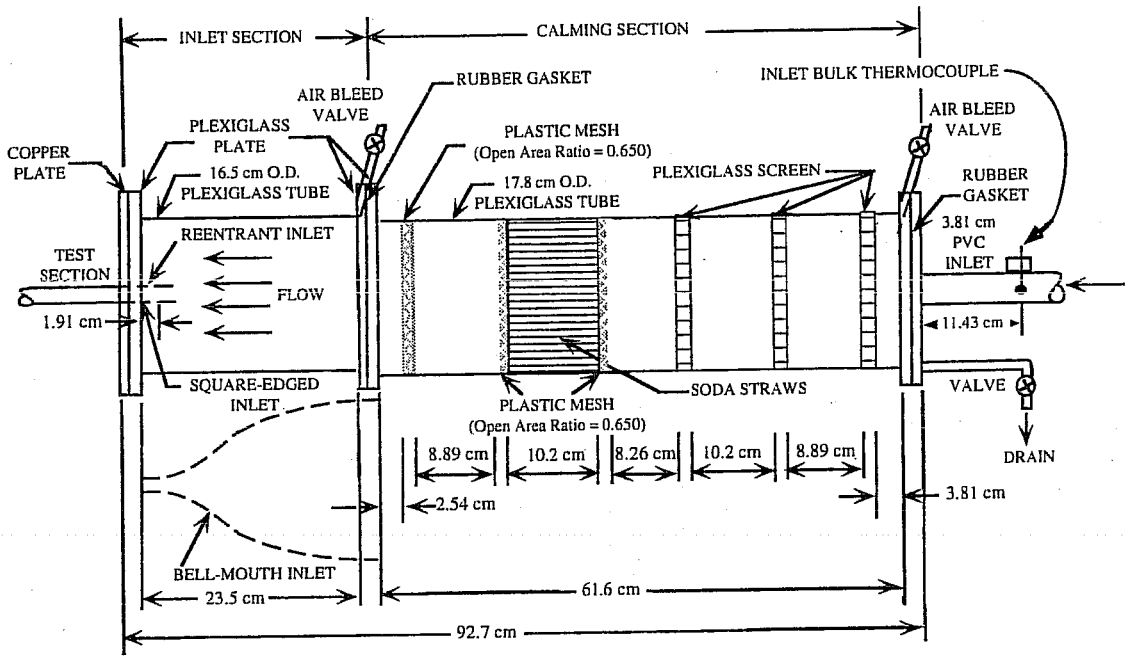

Figure 3. Diagram of calming and inlet sections.

screens were placed at the exit of the calming section. The total length of the calming section is 61.6 cm. Test fluid leaving the calming section entered the inlet section and flowed undisturbed through 23.5 cm of a 16.5-cm-outer-diameter acrylic plastic tube before it entered the test section. This section was added to ensure a uniform velocity distribution upon entering the test section. The calming and inlet sections were also equipped with air bleed valves that were used to evacuate air during start-up.

The inlet section had the versatility of being modified to incorporate a reentrant or a bell-mouth entrance (see Fig. 3). The reentrant entrance was simulated by sliding 1.91 cm of the tube entrance length into the inlet section (Fig. 3), which was otherwise the square-edged (sudden contraction) entrance. For the bell-mouth entrance, a nozzle constructed of fiberglass was used [2]. The nozzle had a contraction ratio of 10.7 and a total length of 23.5 cm.

For nonisothermal pressure drop measurements, a uniform wall heat flux boundary condition was maintained by a Lincoln DC-600 welder. Thermocouples were placed on the outer surface of the tube wall at the fully developed region pressure tap stations 16, 17, and 18. Four thermocouples were used at each station. The thermocouples were placed 90° apart around the periphery. Omega TT-T-30 copper-constantan insulated T-type thermocouples were used with Omega EXPP-T-20 extension wire for relaying the information to the data acquisition system. The thermocouples were attached to the outside of the tube wall with Omegabond 101, an epoxy adhesive with high thermal conductivity and electrical resistivity. The inlet and exit bulk temperatures for isothermal and nonisothermal experiments were measured by using thermocouple probes (Omega TJ36-CPSS-14U-12) inserted in the calming section and the mixing well, respectively. Calibration of thermocouples and thermocouple probes showed that they were accurate to within ± 0.4 °C. The data acquisition system used for the temperature measurements consisted of an Electronic Controls Design model 5100 data logger with 40 input channels interfaced with a personal computer. The flow rate was measured by a turbine meter located upstream from the test section. The turbine meter had a linearity of $\pm 0.5\%$ of reading and a repeatability of less than $\pm 0.10\%$ of reading. The voltage drop across the test section and the current carried by the test section were measured by a voltmeter and an ammeter, respectively.

To investigate the effect of heating on the pressure drop, heat transfer coefficients were measured simultaneously with the friction factors at the same location in the pressure drop test section. The heat transfer measurements at uniform wall heat flux boundary condition were carried out by measuring the local outside wall temperatures at stations 16, 17, and 18 (see Fig. 2) along the axis of the tube and the inlet and outlet bulk temperatures in addition to other measurements such as the flow rate, room temperature, voltage drop across the test section, and current carried by the test section. The local peripheral heat transfer coefficient and Nusselt number were then calculated for each of these stations on the basis of the knowledge of pipe inside wall temperature and inside wall heat flux obtained from a data reduction computer program developed exclusively for this type of experiment [10]. The local average peripheral values for inside wall temperature, inside wall heat flux, heat transfer coefficient, and Nusselt number were then obtained by averaging all the appropriate individual local peripheral values at each axial location. The computer program used a finite-difference formulation to determine the inside wall temperature and the inside wall heat flux from measurements of the outside wall temperature, the heat generation within the pipe wall, and the thermophysical properties of the pipe material (electrical resistivity and thermal conductivity). In these calculations, axial conduction was assumed

negligible (RePr > 42,000, in all cases), but peripheral and radial conduction of heat in the tube wall were included. In addition, the bulk fluid temperature was assumed to increase linearly from the inlet to the outlet. Further details on the heat transfer measurements may be found in Ghajar and Tam [7].

To prevent the welder and the pumps from transmitting noise and vibration through the experimental setup, they were mounted inside a plywood box lined with insulation. Cooling air for the welder was introduced from outside the room to the welder box and exhausted to the exterior of the room through custom-made plenums. In addition, rubber hoses were connected to the pump box to prevent the transmission of vibration to the fluid return tubing. All equipment was placed on damping pads to prevent vibration transmission to the floor.

Various mixtures of ethylene glycol and distilled water were used as the test fluid throughout the experiments to cover the laminar, transition, and turbulent flow regimes. Expressions for the physical properties of ethylene glycol–water mixtures along with their accuracy and range of application are reported in Ghajar and Zurigat [10]. The inlet bulk Reynolds number ranged from about 1000 to 17,000, the local bulk Prandtl number varied from about 6 to 30, the local bulk Grashof number ranged from 0 (isothermal condition) to about 9.65×10^5, and the uniform wall average heat flux ranged from 0 (isothermal condition) to about 16 kW/m^2. Isothermal flow conditions were ensured when the inlet and outlet bulk temperatures were nearly equal (within 0.4 °C of each other). Heat balance errors were calculated for all nonisothermal experimental runs by taking a percent difference between two methods of calculating the heat addition. The product of the voltage drop across the test section and the current carried by the tube was the primary method, and the fluid enthalpy rise from inlet to exit was the second method. The heat balance error between the two methods in all cases was less than 5%. The primary method was the one used in the computer program [10] for all heat transfer calculations.

The reliability of the flow circulation system and the experimental procedures was checked by making several isothermal calibration runs with distilled water and full-strength ethylene glycol, and results were compared with the well-established friction factor correlation of Blasius [3] for fully developed turbulent pipe flow and the fully developed laminar flow equation ($C_f = 16/\mathrm{Re}$). The experimental data were within ±4.5% of the predicted values. The uncertainty analysis of the overall experimental procedures with the use of the method of Kline and McClintock [11] showed that there is a maximum of 5.0% uncertainty for friction factor calculations. Experiments under the same conditions were conducted periodically to ensure the repeatability of the results. The difference between the duplicated experimental runs was within ±5%. A more detailed description of the experimental apparatus and procedures may be found in Tam [12].

EFFECT OF INLET CONFIGURATION ON THE TRANSITION REGION

To investigate the influence of entrance disturbances on the pressure drop transition region, only the isothermal friction factor data for the reentrant, square-edged, and bell-mouth inlets will be analyzed in this section.

Figure 4 clearly shows the influence of inlet configuration on the beginning and end of the pressure drop transition region. This figure plots the fully developed friction factors versus Reynolds number for the three inlets in all flow regimes. Figure 4, for comparison purposes, also shows the established fully developed laminar and turbulent pipe flow friction factor correlations. The solid symbols in the figure represent the start and end of the fully developed transition region for the different inlets. As shown by the solid symbols, the lower and upper limits of the pressure drop transition Reynolds number

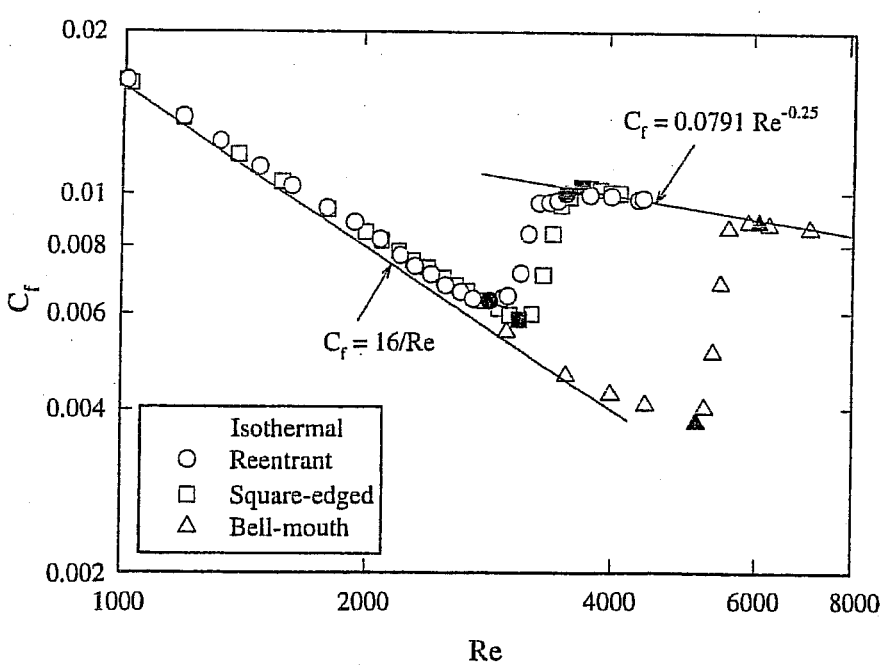

Figure 4. Influence of different inlets on fully developed friction factors. (The solid symbols indicate the start and end of the transition region.)

range are dependent on the inlet configuration. The Reynolds number for the start of the transition region is defined as the Reynolds number corresponding to the first abrupt change in the friction factor, and the Reynolds number for the end of the transition region corresponds to the Reynolds number of the friction factor that first reaches the fully developed turbulent friction factor line. From these data, the limits for the transition Reynolds number range for these three inlet configurations can be summarized as

Reentrant	$2870 < Re < 3500$
Square-edged	$3110 < Re < 3700$
Bell-mouth	$5100 < Re < 6100$.

Because the calming section is a common factor for all three inlets and the flow is isothermal, the difference between the transition Reynolds number ranges is due only to the effect of different inlet configurations. The preceding limits for the friction factor transition Reynolds numbers indicate that the inlet that caused the most disturbance (reentrant) produced an early transition (Re = 2870), and the inlet with the least disturbance (bell-mouth) did not experience transition until a Reynolds number of about 5100. The square-edged inlet, which causes less disturbance than the reentrant inlet but more than the bell-mouth inlet, produced a transition Reynolds number of about 3110. From this observation, it is obvious that the transition Reynolds number range can be manipulated by using different inlet configurations.

EFFECT OF HEATING ON THE TRANSITION REGION

Three different heat fluxes (3, 8, and 16 kW/m^2) were used to investigate the effect of heating on the fully developed friction factor. A DC welder was used to approximate the uniform wall heat flux condition. The results presented in Fig. 5 clearly establish the influence of heating rate. In the laminar and transition regions, heating seems to have a significant influence on the value of friction factor. However, in the turbulent region, heating did not affect the magnitude of the friction factor. The significant influence of heating on the values of friction factor in the laminar and transition regions is directly due to the effect of secondary flow. Application of heat to the tube wall produces a temperature difference in the fluid. The fluid near the tube wall has a higher temperature and lower density than those of the fluid close to the centerline of the tube. This temperature difference is thought to produce a secondary flow owing to free convection. When mixed convection takes place, the velocity profile of the flow changes—in this case, it changes the shear stress and the fluid density of the flow, hence the friction factor is changed. As the heat flux increases, the shear stress due to the change of the velocity profile increases, density becomes smaller, and hence the friction factor increases. To further illustrate the effect of secondary flow, Fig. 6 plots the heat transfer coefficient in terms of Nusselt number (Nu) versus Reynolds number in the laminar flow

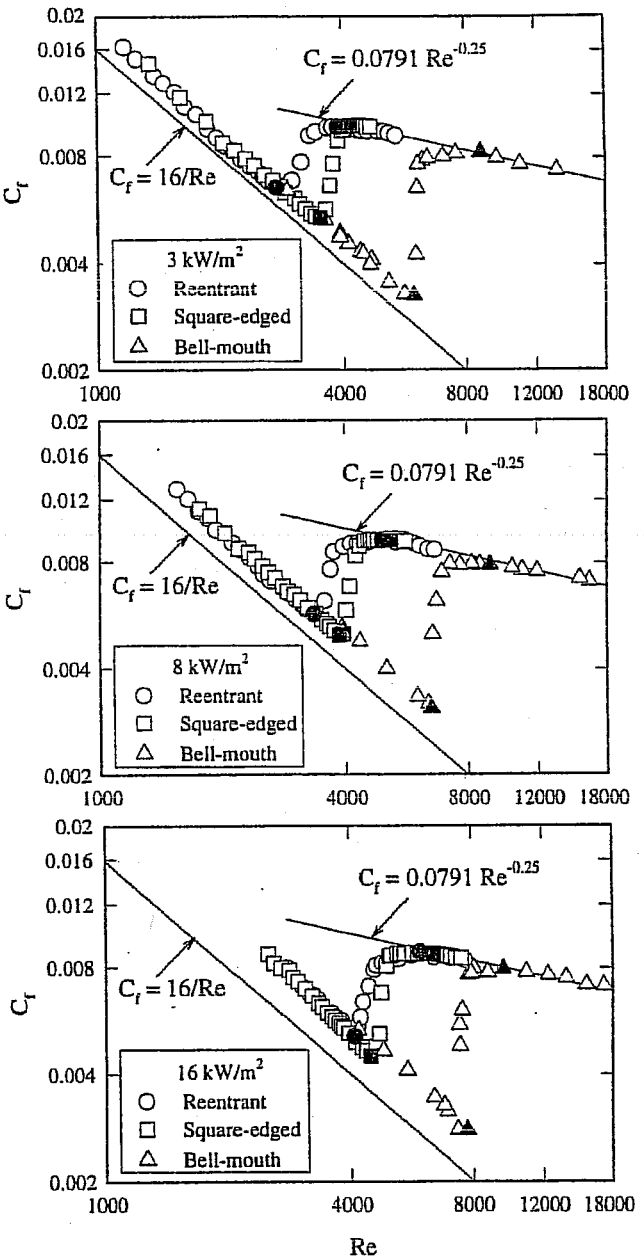

Figure 5. Fully developed friction factors for three different inlets and heat fluxes. (The solid symbols indicate the start and end of the transition region.)

region for the reentrant, square-edged, and bell-mouth inlets under different heat fluxes. These heat transfer coefficients were measured simultaneously with the friction factors at the same location in the pressure drop test section. For comparison purposes, Fig. 6 also shows the typical fully developed pipe flow forced convection heat transfer correlation for laminar flow (Nu = 4.364) under the uniform wall heat flux boundary condition. From the Fig. 6, it can be seen that the data for 3, 8, and 16 kW/m^2 in this flow region follow an almost parallel shift above the accepted laminar heat transfer line. This enhancement is directly due to the strong influence of buoyancy forces on forced convection, giving rise to mixed convection heat

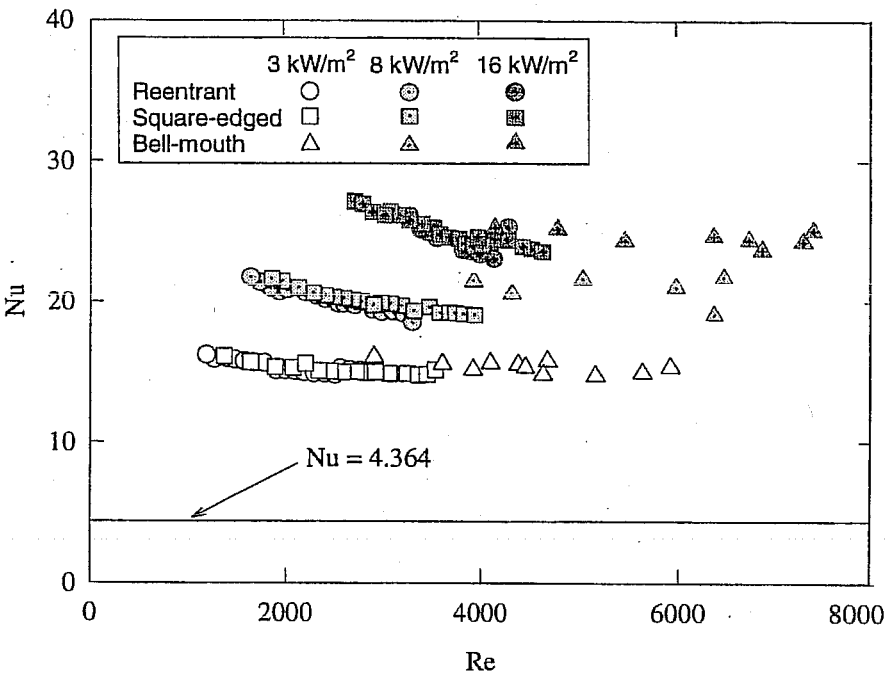

Figure 6. Effect of heating on laminar heat transfer coefficients for the three inlets.

transfer. In the transition region, unlike the laminar region, no such comparisons can be made. To show the effect of secondary flow in the laminar and transition regions, the ratio of local peripheral heat transfer coefficients at the top and bottom of the tube (h_t/h_b) is used. This ratio should be close to unity for forced convection and is much less than unity for a case in which mixed convection exists. Figures 7 and 8 show this heat transfer coefficient ratio versus Reynolds number for the laminar and transition flow regions. Figure 7, for the laminar flow region, shows that, for the same Reynolds number, as heat flux increases, the ratio of the local heat transfer coefficient at the top and bottom of the tube decreases. This trend is consistent with the effect of secondary flow increasing as heat flux increases. In the transition flow region, from Fig. 8, it can be seen that, in all cases, the flow is influenced by secondary flow in the lower transition region (h_t/h_b much less than unity). As Reynolds number increases, the heat transfer coefficient ratio increases and approaches unity in the upper transition region. In the turbulent region, the secondary flow effect is suppressed by the turbulent motion—hence no increase was observed in this region. The transition Reynolds number ranges for the isothermal and nonisothermal (three different heating

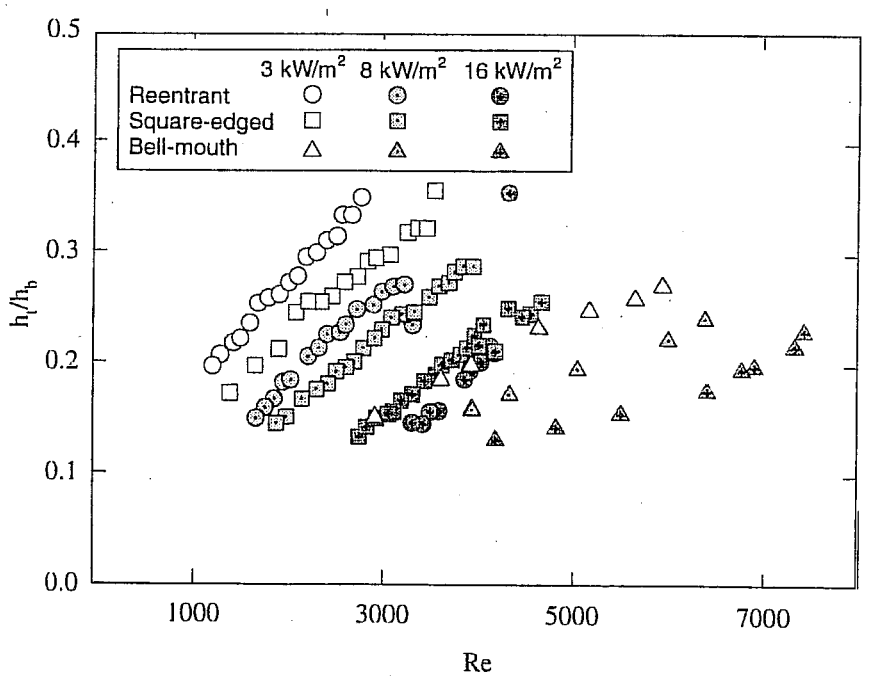

Figure 7. Effect of secondary flow in the laminar region for the three inlets.

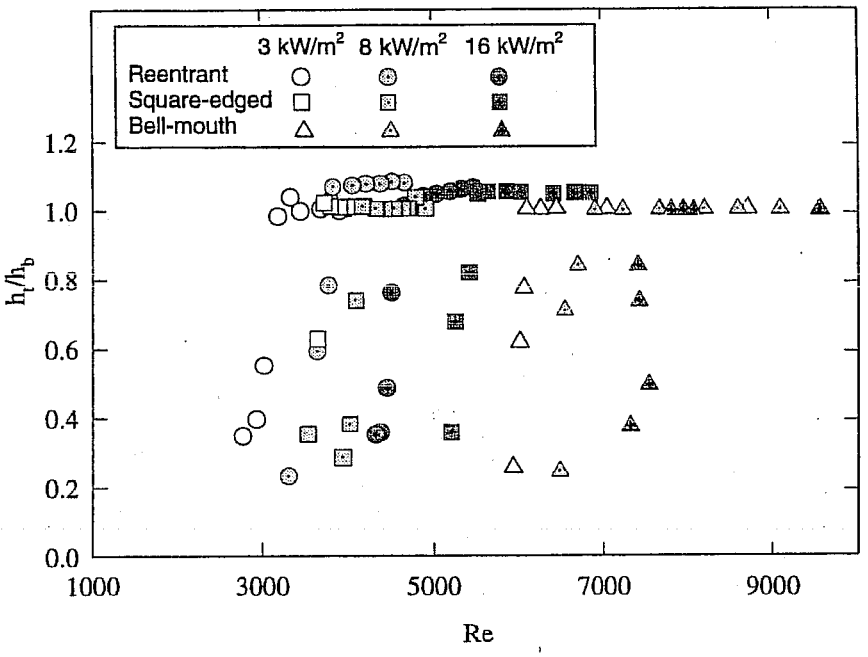

Figure 8. Effect of secondary flow in the transition region for the three inlets.

rates) and the three different inlets used in this study are summarized in Table 2.

The limits for the fully developed friction factor transition Reynolds numbers indicate that both entrance disturbances and heating influence the beginning and end of the transition region. With an increase in the input heat flux for a given inlet configuration, both the upper and the lower limits of the transition Reynolds number increase. The effect of heating is to delay the flow transition or to stabilize the flow and cause the flow to go into transition at a higher Reynolds number.

Figure 5 shows the variation in friction factor under the same heat flux for different inlet configurations. When the heat flux was the same, the most disturbed inlet (reentrant) still produced an early transition. The square-edged inlet, with a disturbance level greater than that of the bell-mouth inlet but less than that of the reentrant inlet, induced transition later than did the reentrant inlet. The bell-mouth inlet, which is the least disturbed inlet, went into the transition last. This behavior is identical with the observations made for the isothermal friction factor (refer to Fig. 4).

COMPARISON OF THE AVAILABLE CORRELATIONS WITH EXPERIMENTS

The experimentally obtained nonisothermal laminar and turbulent fully developed friction factors for the three inlets were compared with the nonisothermal correlations of Test [5], Deissler [4], and Allen and Eckert [6]. These correlations are presented in Table 1.

Figure 9 shows a comparison of our experimental data with the laminar nonisothermal correlation of Test [5]. It can be seen that, for a heat flux of 3 kW/m^2, the agreement between our experimental data and the results predicted by Test's correlation is good (majority of the data were predicted within 10% with an average absolute deviation of 8.5%). However, for heat fluxes of 8 and 16 kW/m^2, Test's correlation underpredicted the experimental data with an average absolute deviation of about -18 to -27%, respectively. The main reason for the underpredictions is the constant value of m (the correction factor) used in Test's correlation. As discussed previously, heating increases the fully developed friction factor, and the exponent m of the correction factor in the isothermal equation is a strong function of the heat flux. With reference to Fig. 5, heating increases the value of the friction factor for a fixed Reynolds number. At low heat flux (3 kW/m^2), the secondary flow effects are not as strong in comparison with the high heat fluxes (8 and 16 kW/m^2); hence, Test's correlation does a good job at these heat fluxes. However, with an increase in the heat flux, the secondary flow effects get stronger and the exponent m is no longer a constant. In Test's correlation, the value of m in the correction factor $1/0.89(\mu_b/\mu_w)^m$ always introduces a correction value close to unity, which is not appropriate with high heat fluxes. Therefore, Test's correlation does

Table 2. Transition Reynolds Numbers

Heat Flux	*Reentrant*	*Square-Edged*	*Bell-Mouth*
0	2870 < Re < 3500	3100 < Re < 3700	5100 < Re < 6100
3 kW/m^2	3060 < Re < 3890	3500 < Re < 4180	5930 < Re < 8730
8 kW/m^2	3350 < Re < 4960	3860 < Re < 5200	6480 < Re < 9110
16 kW/m^2	4090 < Re < 5940	4450 < Re < 6430	7320 < Re < 9560

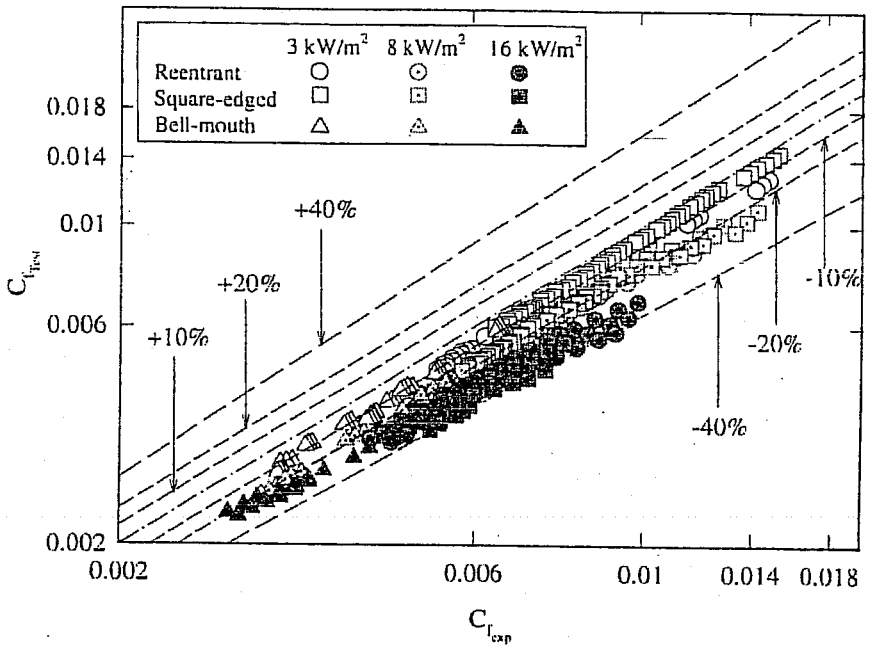

Figure 9. Comparison between experimental fully developed friction factors and laminar correlation of Test [5].

not perform well when strong secondary flow (high heat flux) is involved.

Our experimental data were also compared with the laminar nonisothermal correlation of Deissler [4], as shown in Fig. 10. The comparisons showed that Deissler's correlation underpredicted the experimental data for 3, 8, and 16 kW/m^2, with an average absolute deviation of about -29%, -42%, and -49%, respectively. The deviation increases as the heat flux increases. The main reason, again, is the constant value of m used in the correction factor.

Figure 11 compares our experimental data with the turbulent nonisothermal correlation of Allen and Eckert [6]. For all heat fluxes, Allen and Eckert's correlation did a very good job. A majority of the data (84%) were predicted within 6%, with a maximum deviation of 7.8%. However, in all the turbulent experimental runs, the average of the ratio μ_b/μ_w was equal to 0.86. When the correction factor $(\mu_b/\mu_w)^{-0.25}$ is applied, this correction factor is in fact extremely close to unity. With reference to the discussion on the effect of heating on the friction factor, the turbulent fully developed friction factor for all

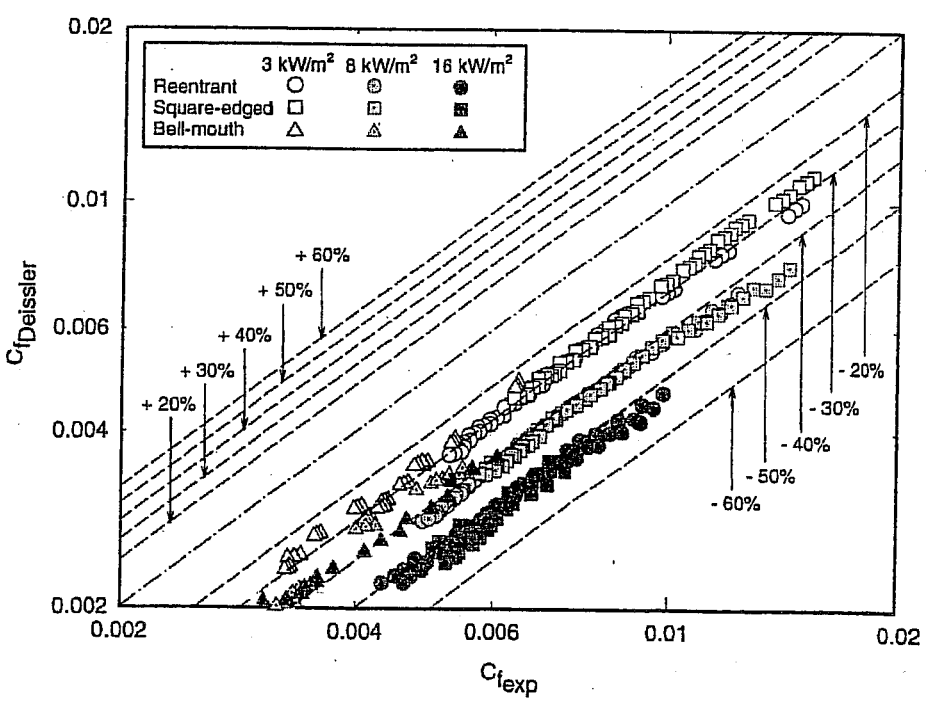

Figure 10. Comparison between experimental fully developed friction factors and turbulent correlation of Deissler [4].

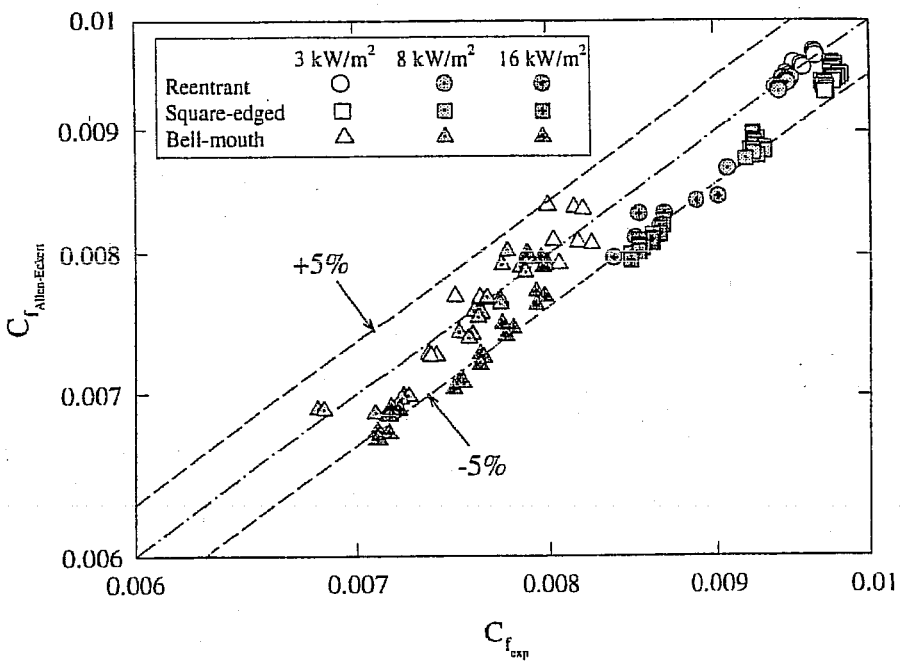

Figure 11. Comparison between experimental fully developed friction factors and turbulent correlation of Allen and Eckert [6].

three different inlets in all three different heat fluxes followed the Blasius correlation extremely well (within ±5%). This means that, in the turbulent region, a correction factor to the established Blasius equation is not necessary.

CORRELATION FOR THE LAMINAR FRICTION FACTOR WITH HEATING

In the laminar region, as pointed out in reference to Figs. 5–7, heating causes an increase in the value of the friction factor owing to the secondary flow effect. Following the form of the classic relation $C_f = 16/\mathrm{Re}$, we applied a correction factor in terms of a viscosity ratio to the laminar isothermal equation to account for the heating effect. The proposed correlation is of the form

$$C_f = \frac{16}{\mathrm{Re}}\left(\frac{\mu_b}{\mu_w}\right)^m, \qquad (2)$$

where $m = 1.65 - 0.013\mathrm{Pr}^{0.84}\mathrm{Gr}^{0.17}$, $1100 < \mathrm{Re} < 7400$, $17{,}100 < \mathrm{Gr} < 95{,}600$, $1.25 < \mu_b/\mu_w < 2.40$, and $6 < \mathrm{Pr} < 36$.

In Eq. (2), the Prandtl and Grashof numbers in the exponent m account for the effect of different heat fluxes on the fully developed laminar friction factor. For the lowest (3 kW/m^2) and the highest (16 kW/m^2) heat fluxes, the correction factor $(\mu_b/\mu_w)^m$ to the isothermal fully developed friction factor varied from about 1.15 to 1.40, respectively. This represents a 15–40% increase in the friction factor over the isothermal value due to different heat fluxes. Equation (2) gives a representation of the experimental data to within +12.1% to −12.6%. In the development of the correlation, a total of 393 experimental data points were used. The absolute average deviation between the results predicted by the correlation and the experimental data is 3%; 80% of the data were predicted with less than 5% deviation; 18% of the data were predicted within 10% deviation. The performance of the proposed correlation at different heat fluxes can be summarized as follows. For low heat flux (3 kW/m^2), the correlation predicts the data with an absolute average deviation of 2.1%. The maximum deviation for this heat flux is 8.2%. For moderate heat flux (8 kW/m^2), the correlation predicts the data with an absolute average deviation of 3.1%. The maximum deviation for this particular heat flux is 11.7%. For high heat flux (16 kW/m^2), the correlation predicts the data with an absolute average deviation of 3.7%. The maximum deviation corresponding to this heat flux is 12.6%. Figure 12 compares the predicted friction factors obtained from the proposed equation with measurements.

CORRELATION FOR THE TRANSITION FRICTION FACTOR WITH HEATING

Because the type of inlet configuration affects the beginning and end of the transition region, a single correlation for this region cannot predict the data, and a correlation for each inlet was developed. The correlation is of the form

$$C_f = \left[1 + \left(\frac{\mathrm{Re}}{a}\right)^b\right]^c \left(\frac{\mu_b}{\mu_w}\right)^m \qquad (3)$$

where the coefficients a, b, c, and m are inlet dependent and were obtained separately for each inlet. The coefficients for each inlet are as follows.

- Reentrant:

$$a = 5840, \quad b = -0.0145, \quad c = -6.23, \quad \text{and}$$

$$m = -1.1 - 0.46\,\mathrm{Gr}^{-0.133}\mathrm{Pr}^{4.1},$$

where $2700 < \mathrm{Re} < 5500$, $16 < \mathrm{Pr} < 35$, $7410 < \mathrm{Gr} < 158{,}300$, and $1.13 < (\mu_b/\mu_w) < 2.13$.

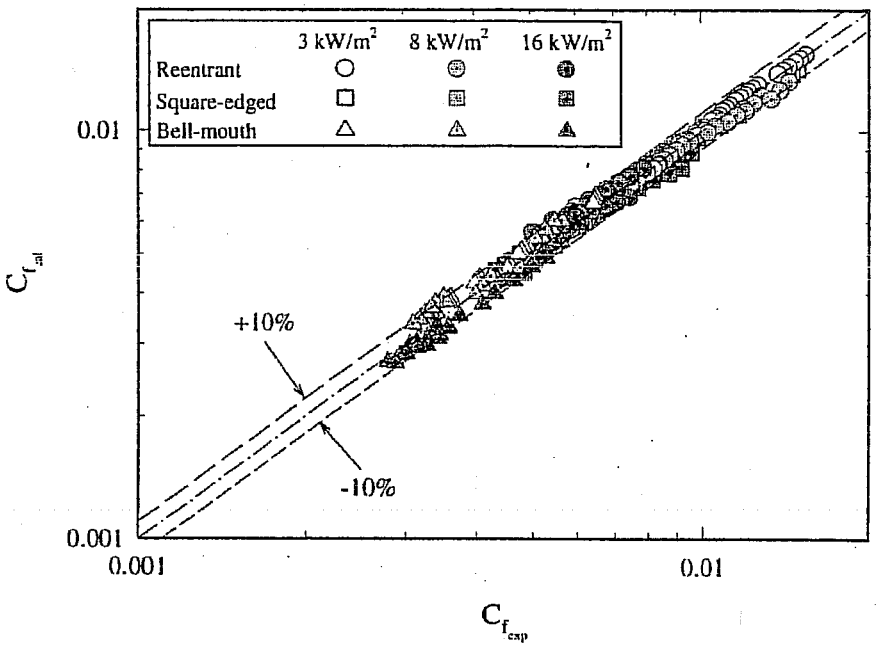

Figure 12. Comparison between experimental fully developed friction factors and the proposed laminar region correlation.

- Square-edged:

$$a = 4230, \quad b = -0.16, \quad c = -6.57, \quad \text{and}$$
$$m = -1.13 - 0.396\,\mathrm{Gr}^{-0.16}\mathrm{Pr}^{5.1},$$

where $3500 < \mathrm{Re} < 6900$, $12 < \mathrm{Pr} < 29$, $6800 < \mathrm{Gr} < 104{,}500$, and $1.11 < (\mu_b/\mu_w) < 1.89$.

- Bell mouth:

$$a = 5340, \quad b = -0.0990, \quad c = -6.32, \quad \text{and}$$
$$m = -2.58 - 0.42\,\mathrm{Gr}^{-0.41}\mathrm{Pr}^{2.46},$$

where $5900 < \mathrm{Re} < 9600$, $8 < \mathrm{Pr} < 15$, $11{,}900 < \mathrm{Gr} < 353{,}000$, and $1.05 < (\mu_b/\mu_w) < 1.47$.

Equation (3) is applicable to a fully developed transition region and should be used with an appropriate set of constants for each inlet configuration. For the development of the transition region correlation for the reentrant inlet, 30 experimental data points were used. The correlation gave a representation of the experimental data to within +9.5% and −9% and had an absolute average deviation of 3.4%. All data for the reentrant inlet were predicted with less than 10% deviation. For the square-edged inlet, 29 experimental data points were used for the development of the correlation. The equation correlated the experimental data to within +20% to −11.8% and had an absolute average deviation of 8.4%; 28% (nine data points) were predicted with ±10–20% deviation, and 72% (21 data points) were predicted with less than ±10% deviation. The correlation for the bell-mouth inlet was based on 24 experimental data points. The correlation represented the experimental data to within +20% to −23% and had an absolute average deviation of 9%; 8%

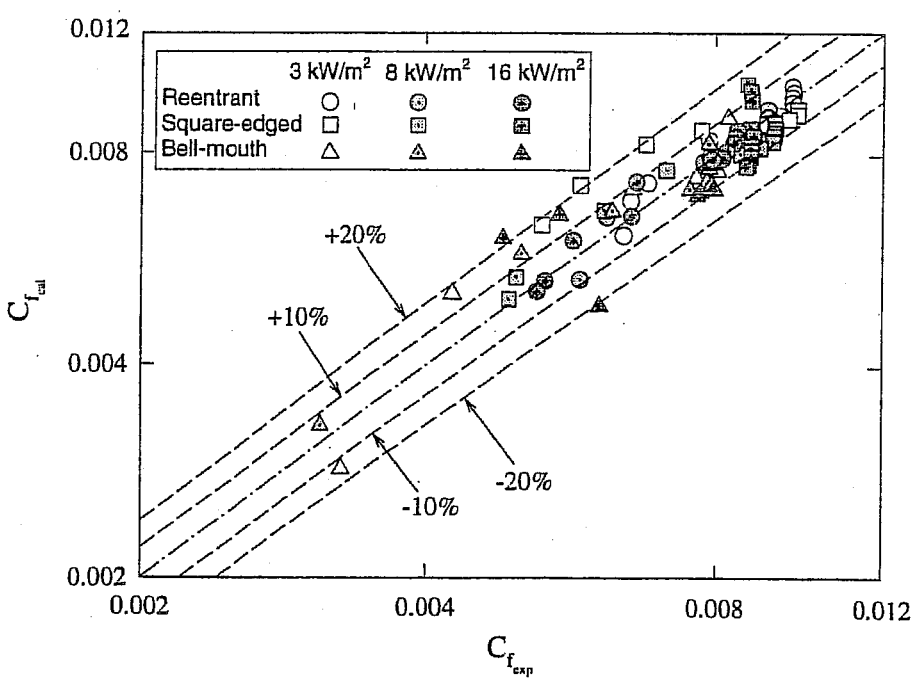

Figure 13. Comparison between experimental fully developed friction factors and the proposed transition region correlation.

(three data points) were predicted with more than ±20% deviation, 20% (five data points) with ±10–20% deviation, and 72% (17 data points) with less than +10% deviation. Figure 13 compares the predicted fully developed friction factor obtained from Eq. (3) for each inlet and different heat fluxes with measurements.

PRACTICAL SIGNIFICANCE

The type of inlet configuration and the rate of heat transfer at the wall (wall heat flux) significantly affect the value of the fully developed friction factor. The friction factor correlations developed in this study can be used to assist heat exchanger designers in predicting the pressure drop along a horizontal straight circular tube with a specified inlet configuration and heat flux in all three flow regimes.

CONCLUSIONS

This study provided an extensive and accurate fully developed isothermal and nonisothermal pressure drop (friction factor) database across all flow regimes for three different inlet configurations. The isothermal friction factors for the three inlets showed that the range of Reynolds number values for which transition flow exists is strongly inlet dependent. Heating caused an increase in the laminar and transitional friction factors and an increase in the lower and upper limits of the isothermal transition region boundaries. The significant influence of heating on the friction factors in the laminar and transition regions was shown to be consistent with the effect of secondary flow.

Comparisons of our laminar nonisothermal friction factor data with nonisothermal laminar correlations showed that the available laminar correlations do not properly account for the effect of heating on the pressure drop. In addition, because heating affects the beginning and end of the transition region, the range of applicability of these correlations is also questionable.

Based on the obtained experimental data, empirical correlations for the prediction of nonisothermal fully developed friction factors in the laminar and transition regions were developed. The correlation developed in this study for the transition region is unique in the sense that there is no other correlation available in the literature for this region. The effect of heating/secondary flow in these correlations was accounted for in terms of a bulk-to-wall-viscosity ratio expressed as a function of Prandtl and Grashof numbers.

NOMENCLATURE

C_f fully developed friction factor ($= \Delta P D / 2 L \rho V^2$), dimensionless
c_p specific heat of the test fluid evaluated at T_b, J/(kg · K)
D inside diameter of test section (tube), m
Gr bulk Grashof number [$= g\beta\rho^2 D^3 (T_w - T_b)\mu^2$], dimensionless
g acceleration of gravity, m/s^2
h fully developed peripheral heat transfer coefficient, W/(m^2 K)
h_b peripheral heat transfer coefficient at the bottom of the tube, W/(m^2 K)
h_t peripheral heat transfer coefficient at the top of the tube (180° from h_b), W/(m^2 K)
k thermal conductivity of the test fluid evaluated at T_b, W/(m K)
L length of the test section (tube), m
m an exponent; see Eq. (1), dimensionless
Nu fully developed peripheral Nusselt number ($= hD/k$), dimensionless
Pr bulk Prandtl number ($= \mu c_p / k$), dimensionless
Re bulk Reynolds number ($= \rho V D / \mu$), dimensionless
T_b bulk temperature of the test fluid, °C
T_w peripheral tube inside wall temperature, °C
V average velocity in the test section, m/s
x distance along the test section from the inlet, m

Greek Symbols

β coefficient of thermal expansion of the test fluid evaluated at T_b, K^{-1}
ΔP pressure difference, Pa
μ_b absolute viscosity of the test fluid evaluated at T_b, Pa s
μ_w absolute viscosity of the test fluid evaluated at T_w, Pa s
ρ density of the test fluid evaluated at T_b, kg/m^3

Subscripts

cal. refers to the calculated value
cp refers to the isothermal (constant-property) value
exp refers to the experimental value
vp refers to the nonisothermal (variable-property) value

REFERENCES

1. Kakac, S., The Effect of Temperature-Dependent Fluid Properties on Convective Heat Transfer. In *Handbook of Single-Phase Convective Heat Transfer*, S. Kakac, R. K. Shah, and W. Aung, Eds., Chap. 18, Wiley-Interscience, New York, 1987.
2. Ghajar, A. J., and Madon, K. F., Pressure Drop Measurements and Correlations in the Transition Region for a Circular Tube with Three Different Inlet Configurations. *Exp. Thermal Fluid Sci.* **5**, 129–135, 1992.
3. Blasius, H. Das Ähnlichkeitsgesetz bei Reibungsvorgängen in Flüssigkeiten. *Forsch. Arb. Ing.-Wes.* 131, 1913.
4. Deissler, R. G., Analytical Investigation of Fully Developed Laminar Flow in Tubes with Heat Transfer with Fluid Properties Variable Along the Radius. NACA TN 2410, Washington, DC, 1951.
5. Test, F. L., Laminar Flow Heat Transfer and Fluid Flow for Liquids with Temperature-Dependent Viscosity. *J. Heat Transfer* **90**, 385–393, 1968.
6. Allen, R. W., and Eckert, E. R. G., Friction and Heat Transfer Measurements to Turbulent Pipe Flow of Water (Pr = 7 and 8) at Uniform Wall Heat Flux. *J. Heat Transfer* **86**, 301–310, 1964.
7. Ghajar, A. J., and Tam, L. M., Heat Transfer Measurements and Correlations in the Transition Region for a Circular Tube with Three Different Inlet Configurations. *Exp. Thermal Fluid Sci.* **8**, 79–90, 1994.
8. Ghajar, A. J., and Tam, L. M., Flow Regime Map for a Horizontal Pipe with Uniform Wall Heat Flux and Three Inlet Configurations. *Exp. Thermal Fluid Sci.* **10**, 287–297, 1995.

9. Kong, S. C., Tam, L. M., and Ghajar, A. J., Intermittency Factor Measurements in the Transition Region for a Circular Tube with Two Different Inlet Configurations. Presented at the AIAA 24th Fluid Dynamics Conference, Orlando, FL, AIAA Paper No. 93-3073, July 6–9, 1993.
10. Ghajar, A. J., and Zurigat, Y. H., Microcomputer-Assisted Heat Transfer Measurement/Analysis in a Circular Tube. *J. Appl. Eng. Educ.* 7, 125–134, 1991.
11. Kline, S. J., and McClintock, F. A., Describing Uncertainties in Single Sample Experiments. *Mech. Eng.* 1, 3–8, 1953.
12. Tam, L. M., An Experimental Investigation of Heat Transfer and Pressure Drop in the Transition Region for a Horizontal Tube with Different Inlets and Uniform Wall Heat Flux. Ph.D. Thesis, School of Mechanical and Aerospace Engineering, Oklahoma State Univ., Stillwater, OK, 1995.

Received September 5, 1996; revised December 30, 1996